



## $^{60}\text{Co}$ gamma irradiation effects on electrical characteristics of $\text{Al}/\text{Y}_2\text{O}_3/\text{n-Si}/\text{Al}$ capacitors

Minh-Tri TA, David Briand \*, Bertrand Boudart, Yannick Guhel

Laboratoire Universitaire des Sciences Appliquées de Cherbourg (LUSAC), EA 4253, Université de Caen Basse-Normandie, BP 78, 50130 Cherbourg Octeville, France

### ARTICLE INFO

#### Article history:

Received 31 March 2009

Received in revised form 18 December 2009

Accepted 24 January 2010

Available online 28 January 2010

#### Keywords:

Gamma irradiation

MOS structure

Yttrium oxide

Thermal annealing

### ABSTRACT

$\text{Al}/\text{Y}_2\text{O}_3/\text{n-Si}/\text{Al}$  capacitors were irradiated by using a  $^{60}\text{Co}$  gamma ray source and a maximum dose up to 8.4 kGy. The effect of an annealing treatment performed at 600 or 900 °C on the yttrium oxide ( $\text{Y}_2\text{O}_3$ ) films was investigated by XRD and Raman spectroscopy. High-frequency capacitance–voltage ( $C-V$ ) and conductance–voltage ( $G-V$ ) measurements as well as quasi-static measurements of the MOS structures were analysed. The annealing improves the crystalline state of the  $\text{Y}_2\text{O}_3$  thin film material and decreases the values of the flat-band voltage and of the interface trap level density indicating an improvement of the electrical properties of the interface thin film–substrate. But at this interface, the formation of an yttrium-silicate layer was also evidenced. After gamma irradiation, the values of the flat-band voltage and of the interface trap level density related to the  $\text{Al}/\text{Y}_2\text{O}_3/\text{n-Si}/\text{Al}$  structure increase and especially for the structure made with the materials annealed at 900 °C for 1 h. In that case, the structure is very sensitive to a gamma irradiation dose up to 8.4 kGy.

© 2010 Elsevier B.V. All rights reserved.

### 1. Introduction

The interfacial layer formed between high- $k$  oxides and silicon in a MOS structure plays a major role in the expected dielectric properties as well as in the behaviour of the device. Moreover, when these devices are exposed to high-level radiation such as gamma radiation, significant changes can be occurred in the electrical characteristics of the device.

The studies of the modification in semiconductor devices due to irradiation are of both technological importance and scientific interest [1,2]. Generally, the exposure of these devices to high-energy particles results in displacement lattice damage and ionisation damage which can create free charges in the material [3]. These damages can have an impact on the electrical properties of the devices and consequently on their performances. The effect of gamma radiation on high- $k$  oxide in MOS structures has been studied in the past [4] and is still studied now [5].

Among the high- $k$  oxides, yttrium oxide ( $\text{Y}_2\text{O}_3$ ) has attracted a lot of attention in the past because of several physical properties relevant for MOS devices. This oxide can be grown on Si using different methods like r.f. magnetron sputtering [6], electron-beam evaporation [7], laser ablation [8], ion beam sputtering [9], and epitaxy [10]. The interest in  $\text{Y}_2\text{O}_3$  to replace  $\text{SiO}_2$  in MOS devices has decreased, due to its relatively medium  $k$  value (less than 20)

and the formation of a low  $k$  value interfacial layer, but no results are reported concerning its gamma radiation hardness.

To fill this gap, we report on effects of  $^{60}\text{Co}$   $\gamma$ -ray irradiation on the electrical characteristics of  $\text{Al}/\text{Y}_2\text{O}_3/\text{n-Si}/\text{Al}$  capacitors exposed at room temperature to a cumulative dose up to 8.4 kGy.

### 2. Experiments

$\text{Al}/\text{Y}_2\text{O}_3/\text{n-Si}/\text{Al}$  structures were fabricated on n-type Si semiconductor wafers with (1 1 1) orientation, 350  $\mu\text{m}$  thickness and 0.01–0.05  $\Omega\text{ cm}$  resistivity. Before the growth the Si wafers were chemically cleaned using the RCA cleaning procedure. The native oxide on the front surface was removed in a diluted HF solution (1 mol/L), rinsed in deionized water for a prolonged time and dried with  $\text{N}_2$ . Immediately after the cleaning procedure, the wafers were introduced in a vacuum system equipped with a water-cooled r.f. magnetron sputtering gun operating at 13.56 MHz. The system was initially pumped to  $10^{-4}$  Pa. Argon and oxygen were used as sputtering gas and were introduced in the chamber with a gas flow of  $83 \times 10^{-3}$  and  $3.32\text{ Pa m}^3\text{ s}^{-1}$ , respectively. The r.f. magnetron power was chosen to 50 W and the anode–cathode distance was adjusted to 3 cm. The yttrium metal solid targets used in this work were manufactured with a nominal purity of 99.99%. The substrate temperature was fixed at 600 °C and the growth time lasted 1 h. The thickness  $d_{\text{ox}}$  of the  $\text{Y}_2\text{O}_3$  films, measured by profilometer, is  $125 \pm 5\text{ nm}$ .

A post growth annealing was performed in an oven under a dry secondary vacuum ( $10^{-6}$  torr) in the temperature range

\* Corresponding author. Tel.: +33 2 33 01 42 20; fax: +33 2 33 01 41 35.  
E-mail address: [david.briand@unicaen.fr](mailto:david.briand@unicaen.fr) (D. Briand).

600–900 °C, for 1 h. A 300 nm thick aluminium layer was evaporated at  $10^{-6}$  torr on the oxide surface. Square dots with an elementary surface (A) of  $4.225 \times 10^{-3} \text{ cm}^2$  were defined by etching Al and oxide with a diluted  $\text{H}_3\text{PO}_4$  solution. The back side of the wafers was also metallized in the same way.

All the deposited thin films were characterized by X-ray Diffraction (XRD) and by Raman spectroscopy. An X-ray diffractometer (SIEMENS D5005) was employed for crystal phase measurement using a scan range of  $20^\circ$ – $65^\circ$  ( $2\theta$ ). A step size and a scan speed of  $0.01^\circ$  ( $2\theta$ ) were implemented with 3 s per step, respectively. The Cu  $K\alpha$  radiation  $\lambda = 1.5418 \text{ \AA}$  was run under a voltage of 40 kV and a current of 30 mA. Diffractograms were collected in Bragg–Brentano ( $\theta$ – $2\theta$ ) geometry. Raman spectra were recorded in a backscattering configuration at room temperature with an InVia RENISHAW Raman spectrometer. An argon-ion laser with a wavelength of 514.5 nm was used as the excitation source to analyse the different thin layers. A  $50\times$  objective was used.

The C–V and G–V measurements of  $\text{Al}/\text{Y}_2\text{O}_3/n\text{-Si}/\text{Al}$  capacitors were performed at room temperature and in the dark with a HP 4192A LF impedance analyser before and after each gamma irradiation. Voltage was swept from inversion to accumulation regime [11], using a step of 0.2 V and a sweep rate of  $50 \text{ mV s}^{-1}$ . The value of the oscillator level was fixed at 0.9 V so that our probe station was accurately calibrated in the frequency range 0.0002–1 MHz. A HP 4155C semiconductor parameter analyser was also used to perform quasi-static measurements.

Irradiations were carried out at room temperature and with a dose rate of 25 Gy/h using a  $^{60}\text{Co}$  radiation source in irradiation facilities of the INSTN in Cherbourg. The maximum cumulative dose was 8.4 kGy.

### 3. Results and discussion

#### 3.1. Physical analysis

Fig. 1(a) shows the XRD pattern of  $\text{Y}_2\text{O}_3$  thin film deposited at 600 °C on a (1 1 1) Si substrate and annealed at 900 °C for 1 h. In this figure, we only show two different peaks located at  $28.3^\circ$  and  $29.0^\circ$ . In accordance with the Joint Committee on Powder Diffraction Standards files, they are attributed to a (1 1 1) plane for the Si substrate (JCPD 027-1402) and to a (2 2 2) plane for the  $\text{Y}_2\text{O}_3$  thin film (JCPD 041-1105), respectively. It proves that as-deposited and annealed film is strongly (1 1 1) oriented. This phenomenon was also observed by Evangelou et al. [12] and Fukumoto et al. [13]. Fig. 1(b) shows the evolution of the position and of the full-width at half-maximum (FWHM) of the peak corresponding to  $\text{Y}_2\text{O}_3$  before and after annealing. The position of the peak does not change. On the other hand, FWHM strongly decreases versus the annealing temperature. That indicates that the annealing treatment really ameliorates the crystallinity of the film without any change of the stress of the film towards the substrate. This is in accordance with the study of Cheng et al. [14].

Fig. 2 presents the comparison of Raman spectra of a Si(1 1 1) substrate and of  $\text{Y}_2\text{O}_3$  layers deposited on Si(1 1 1) wafer before and after annealing performed at 600 and 900 °C for 1 h. We can observe two Raman lines located at  $320.0$  and  $436.5 \text{ cm}^{-1}$  which correspond to the longitudinal optical mode of the Si substrate [15]. An additional peak located at  $376.0 \text{ cm}^{-1}$  is clearly evidenced for high annealing temperature. It corresponds to the triply degenerate Raman active mode of the  $\text{Y}_2\text{O}_3$  thin film [16]. We can also observe some shoulders evidenced at high annealing temperature by the dashed circles in Fig. 2. They are attributed to amorphous yttrium-silicate layer present at the interface between  $\text{Y}_2\text{O}_3$  and Si.

Fig. 3 shows the SEM image of a surface of  $\text{Y}_2\text{O}_3$  thin film grown at 600 °C on a Si(1 1 1) substrate. The part on the right side which

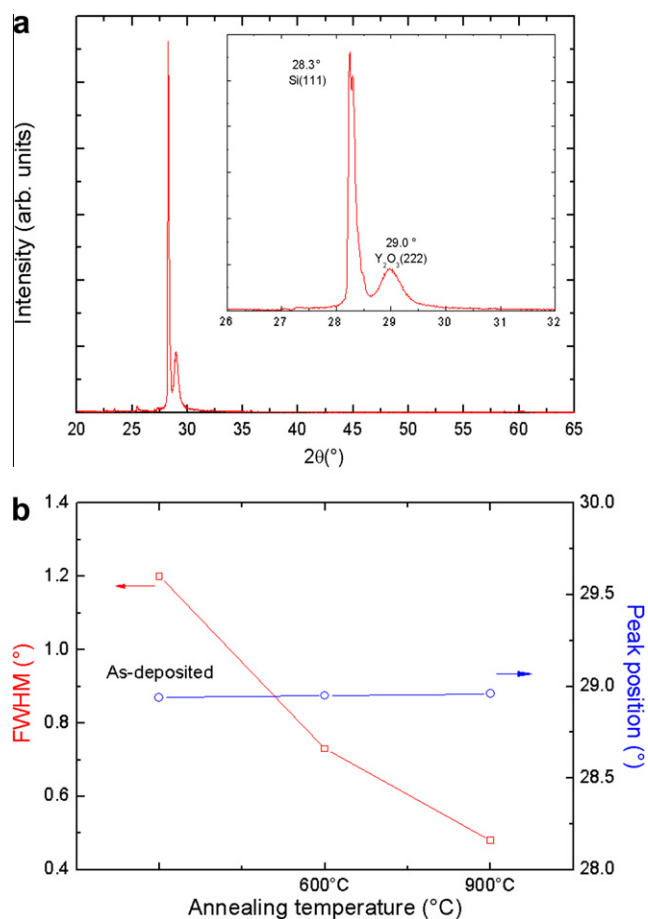


Fig. 1. X-ray diffraction pattern of  $\text{Y}_2\text{O}_3$  thin film grown on Si(1 1 1) by r.f. magnetron sputtering (a) and evolution of the position and of the FWHM (b) of the  $\text{Y}_2\text{O}_3$  related peak before and after annealing performed at different temperatures.

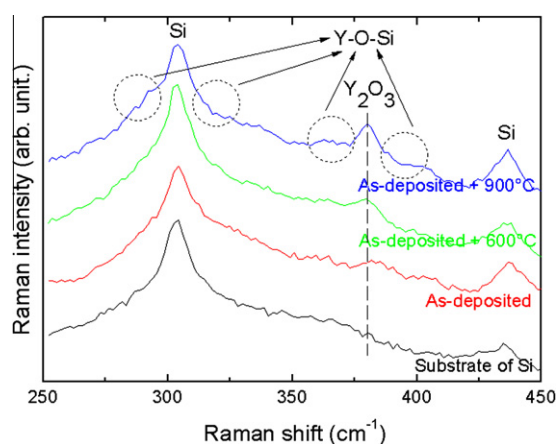
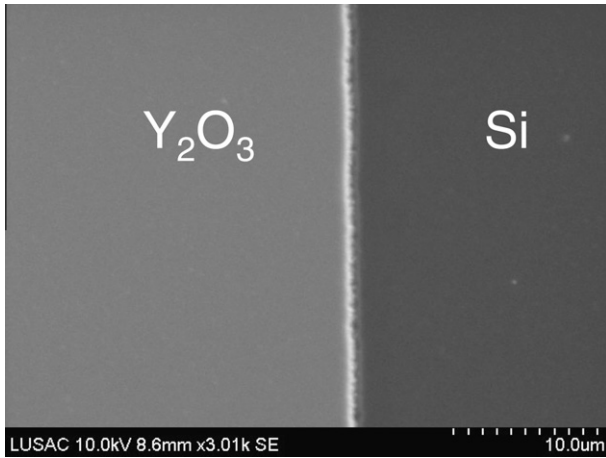


Fig. 2. Raman spectra of a Si(1 1 1) wafer and of  $\text{Y}_2\text{O}_3$  thin film grown on Si(1 1 1) before and after annealing performed at different temperatures.

shows the Si surface was obtained after etching the oxide. The vertical white line is the boarder the both parts. The surface of the film is smooth and shows no evidence of pitting. The films grown at 600 °C and post growth annealed at different temperatures (600 or 900 °C) were also observed and we did not notice any difference.



**Fig. 3.** SEM image of an as-deposited  $\text{Y}_2\text{O}_3$  thin film grown at 600 °C on a Si(1 1 1) substrate.

### 3.2. Electrical characterization

#### 3.2.1. Unirradiated capacitors

Fig. 4(a) and (b) show respectively quasi-static and high-frequency (1 MHz) C–V measurements of  $\text{Al}/\text{Y}_2\text{O}_3/\text{Si}/\text{Al}$  structures, carried out on as-deposited thin film or after a post growth annealing performed at 600 or 900 °C, during 1 h.  $C/C_{\text{ox}}$  is the normalized

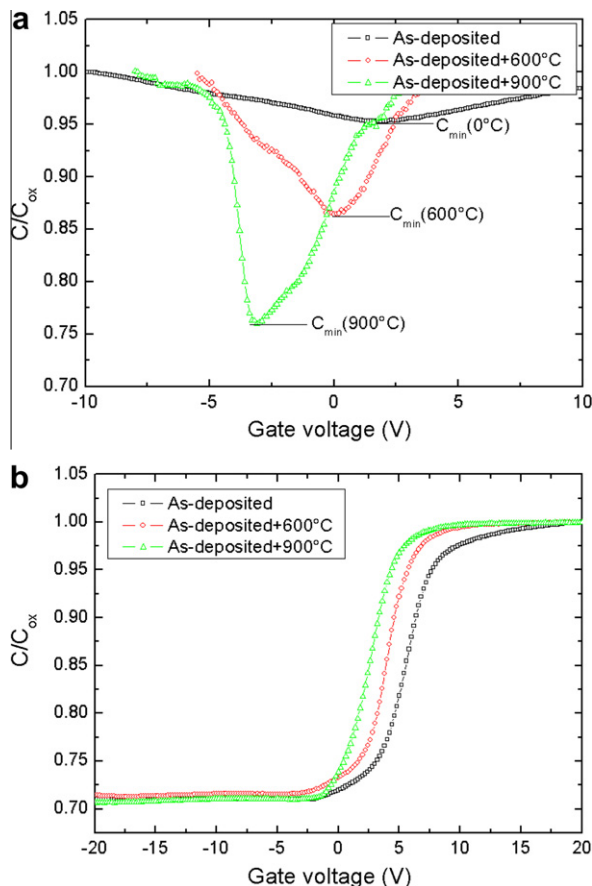


**Fig. 4.** Capacitance–voltage characteristics of  $\text{Al}/\text{Y}_2\text{O}_3/\text{Si}/\text{Al}$  structures carried out on as-deposited thin film or after a post growth annealing performed at 600 or 900 °C, during 1 h measured by quasi-static method (a) and high-frequency at 1 MHz (b).

capacitance and  $C_{\text{ox}}$  is the capacitance in accumulation. The minimum low frequency capacitance decreases after annealing and the corresponding voltage is shifted towards negative values. These are the symptoms of an interfacial charge nonuniformity, but could also be caused by interface traps [17]. Two effects of the annealing were also observed on the high-frequency curves. The visible stretchout of the as-deposited sample curve, due to high density of interface trap, is reduced or eliminated after thermal treatment and the curve is shifted towards negative values, indicating a change of the oxide charge density. In both cases, these effects are more pronounced when the annealing temperature is high. These observations can be correlated with the physical analysis which indicates an improvement of the crystalline state of the oxide after annealing. We think that the thermal treatment reduces the interface trap density as well as the charge nonuniformity at the interface, and that the oxide charge density in the bulk is simultaneously decreased. It is attributed to the recovery of structural defects such as broken bonds and oxygen vacancies, in the bulk as well as at the interface.

The dielectric constant of the oxide layer was calculated from high-frequency data (Fig. 4(b)), using the following equation:

$$C_{\text{ox}} = \frac{A\epsilon_0\epsilon_{\text{ox}}}{d_{\text{ox}}} \quad (1)$$

where  $C_{\text{ox}}$  is the value of the capacitance in the accumulation region,  $A$  is the effective area of the capacitance,  $\epsilon_0$  is the absolute permittivity,  $\epsilon_{\text{ox}}$  is the dielectric constant of the oxide, and  $d_{\text{ox}}$  is the thickness of the oxide.

From Eq. (1), the dielectric constant of the  $\text{Y}_2\text{O}_3$  as-deposited thin film has been estimated to  $14.5 \pm 1.5$  for different capacitors realized on the same wafer. This variation is due to film inhomogeneities. These values are higher than those obtained by Lee et al. [18] or by Yip and Shih [19], and are in accordance with the Horng's et al. [6] and Evangelou's et al. [12] studies. Fig. 5(a) shows that the dielectric constant value decreases after annealing. The calculation of the dielectric constant, which is a bulk property, takes into account the  $\text{Y}_2\text{O}_3$  material but also the interfacial yttrium-silicate layer that Raman analysis has evidenced after annealing. This layer has a lower dielectric constant value. Since we concluded from RX diffraction and high-frequency measurements that the oxide layer has better structural and electrical properties after the thermal treatment, this evolution of the dielectric constant can be explained only by the presence of the yttrium-silicate layer. To verify it, a 30 nm thick sample has been deposited. Its dielectric constant is about 10 and does not vary significantly after annealing. It indicates clearly the existence of the yttrium-silicate layer, which drastically affects the dielectric constant for low thicknesses samples.

Measurement of the interface trap level density ( $D_{\text{it}}$ ) at the  $\text{Y}_2\text{O}_3/n\text{-Si}$  interface is a useful guide to value the quality of the MOS capacitor [17]. To determine the interface trap level density, various measurement techniques such as high–low frequency capacitance [20] or quasi-static capacitance [21] have been developed. In this study,  $D_{\text{it}}$  was extracted from both C–V and G–V curves according to the convenient single-frequency approximation proposed by Hill and Coleman [22], using the following relation:

$$D_{\text{it}} = \frac{2}{qA} \frac{\frac{C_{\text{max}}}{\omega}}{\left(\frac{C_{\text{max}}}{\omega C_{\text{ox}}}\right)^2 + \left(1 - \frac{C_{\text{max}}}{C_{\text{ox}}}\right)^2} \quad (2)$$

where,  $A$  and  $C_{\text{ox}}$  were defined in the first equation,  $\omega$  is the angular frequency,  $q$  is the elementary electrical charge,  $C_{\text{max}}$  conforms to the maximum of G–V curve (this maximum, not shown here, is associated to the losses due to the exchange between interface defects and the semiconductor), and  $C_{\text{max}}$  is the capacitance corresponding to  $G_{\text{max}}$ .

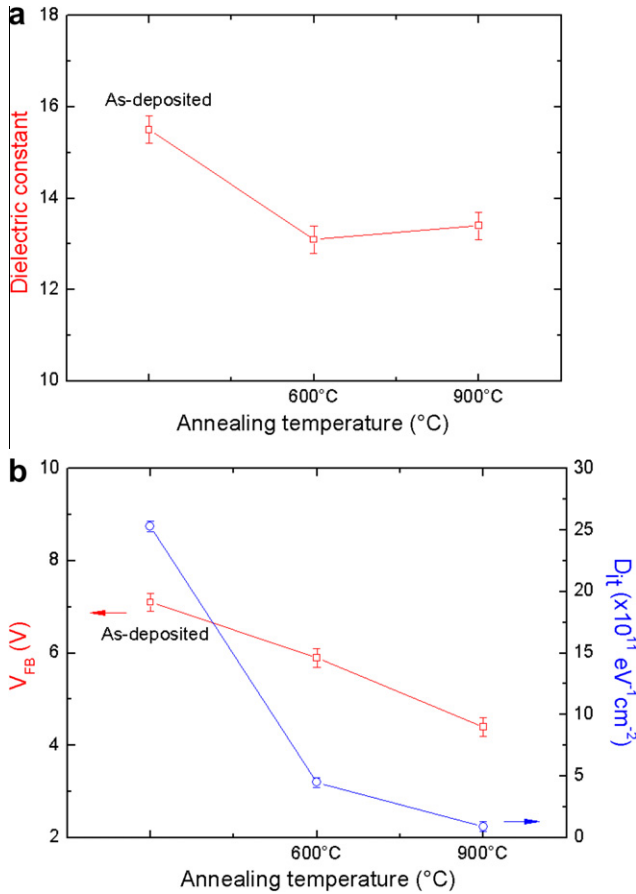


**Fig. 5.** Variation of the dielectric constant (a) and of the flat-band voltage and of the interface trap level density (b) versus annealing temperature.

From Eq. (2),  $D_{it}$  can be calculated to  $2.5 \times 10^{12} \text{ eV}^{-1} \text{ cm}^{-2}$  before annealing. This value is higher than other values ( $2\text{--}9 \times 10^{11} \text{ eV}^{-1} \text{ cm}^{-2}$ ) obtained for Y<sub>2</sub>O<sub>3</sub>/Si structure [18,23]. This divergence can be explained by the fact that the orientation of the substrates are different, (1 1 1) in our case and (1 0 0) for the other.

Fig. 5(b) shows the evolution of the flat-band voltage and of the interface trap density before and after an annealing treatment performed at 600 or 900 °C for 1 h. We can observe that  $V_{FB}$  and  $D_{it}$  decrease after annealing due to an improvement of the crystalline quality of the structure, in the bulk as well as at the interface [17].

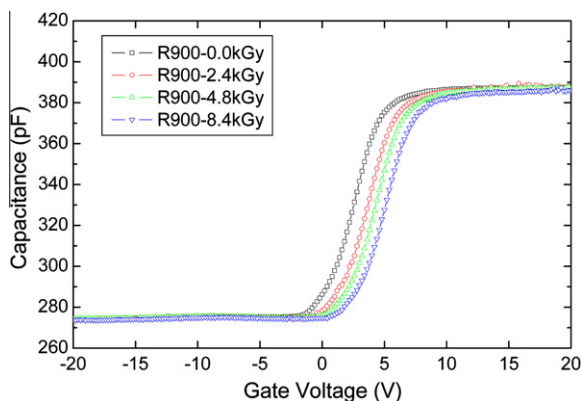


**Fig. 6.** High-frequency (1 MHz) C-V characteristics of the post growth annealed at 900 °C Al/Y<sub>2</sub>O<sub>3</sub>/Si/Al structure for different gamma irradiation doses.

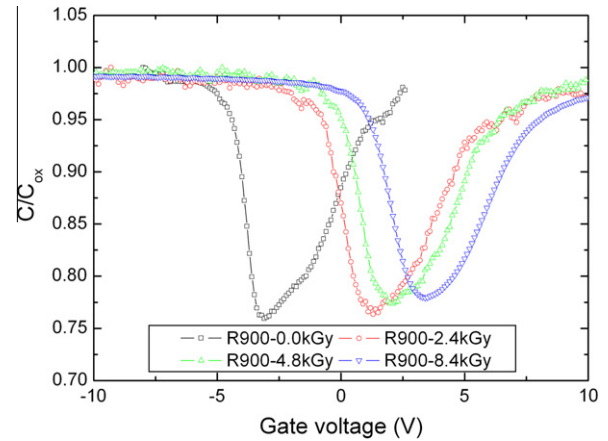


**Fig. 7.** Quasi-static C-V characteristics of Al/Y<sub>2</sub>O<sub>3</sub>/Si/Al structure before and after gamma irradiation.

### 3.2.2. Radiated capacitors

Sample annealed at 900 °C has the better electrical characteristics (i.e. lower  $D_{it}$  and  $V_{FB}$ ). Fig. 6 shows its high-frequency (1 MHz) capacitance-voltage (C-V) curves before and after irradiation with cumulative dose of 2.4, 4.8, and 8.4 kGy. The C-V curve moves towards the positive voltage when the irradiation dose increases. This shift, connected to a degradation of the bulk material, is probably due to the creation of trapped negative oxide charges in the Y<sub>2</sub>O<sub>3</sub> thin layer, as reported in the literature [5]. The quasi-static

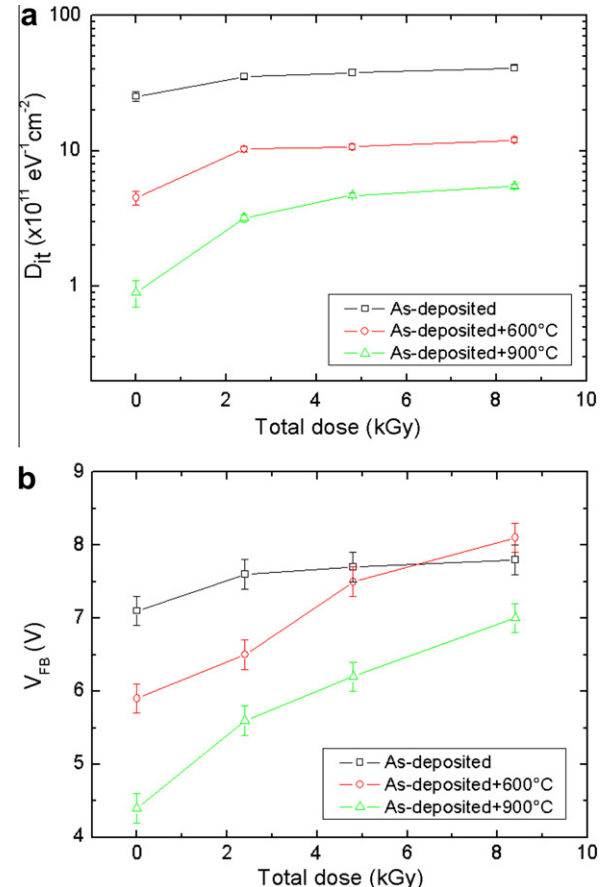


**Fig. 8.** Variation of the interface trap level density (a) and of the flat-band voltage (b) versus irradiation dose.



capacitance–voltages curves are reported in Fig. 7. The gamma radiation causes the curve to move towards the positive voltage, however the minimum low frequency capacitance does not change significantly, as observed in Fig. 4(a).

Fig. 8(a) presents the evolution of  $D_{it}$  calculated from Eq. (2) with irradiation for different annealing conditions. For all the samples,  $D_{it}$  strongly increases with the irradiation dose. The maximum relative variation of  $D_{it}$  were calculated according the formula:

$$\Delta D_{it} = \frac{D_{it}^{\min} - D_{it}^{\max}}{D_{it}^{\min}} \times 100(\%) \quad (3)$$

where,  $D_{it}^{\min}$  and  $D_{it}^{\max}$  are respectively the interface trap densities before irradiation and for the maximum dose. Their values are: 63% for the as-deposited sample, 166% for the sample annealed at 600 °C and 511% for that annealed at 900 °C. The variation of the flat-band voltage  $V_{FB}$  is shown in Fig. 8(b). The maximum relative variations of  $V_{FB}$  for the three capacitors are respectively 10%, 37% and 60%. It demonstrates that better are the crystalline quality of the structure (in the bulk as well as at the interface  $Y_2O_3/Si$ ), more the structures are sensitive to gamma radiation.

Similar experiments were carried out on a 30 nm thick sample annealed at 900 °C.  $\Delta D_{it}$  was found to be 334%, but the flat-band voltage did not vary after irradiation. This could indicate that  $Y_2O_3$  is not so much sensitive to gamma ray, and that the film must be enough thick to modify the oxide charge. In comparison to some others high- $k$  oxides, Zhao et al. [5] have recently studied the response of gamma ray radiation of  $HfO_2$  and  $ZrO_2$  on 16 nm thick layer and found a dielectric degradation by measurement of  $V_{FB}$ , as well as an increase of the interface state density.

#### 4. Conclusion

In a first step, we have studied the effect of an annealing treatment performed at 600 or 900 °C for 1 h on  $Y_2O_3$  films used in Al/ $Y_2O_3/n$ -Si/Al structures. After annealing, the improvement of the quality of the  $Y_2O_3$  thin film material has been evidenced by XRD. At this interface, the formation of an yttrium-silicate layer has also been evidenced by Raman spectroscopy. Its influence on the dielectric constant of thin deposited layer is strong. In the same time,  $D_{it}$  and  $V_{FB}$  have strongly decreased after the treatment indicating an improvement of the electrical properties in the bulk and at the interface thin film–substrate.

In a second step, the influence of a  $\gamma$ -ray radiation on the electrical characteristics of the MOS capacitors has been studied. We have shown that the interface trap level density is very sensitive to a gamma irradiation dose up to 8.4 kGy, and especially for the structure made with the materials annealed at 900 °C for 1 h. It is true also for the flat-band voltage, provided that the yttrium oxide film is enough thick.

#### Acknowledgements

The authors would like to acknowledge the financial support of the Région Basse-Normandie and of the “Syndicat Mixte du Cotentin”. The authors would also like to thank A. Pin at “Institut National des Sciences et Techniques Nucléaires” (INSTN-CEA) in Cherbourg for the assistance with the gamma irradiation.

#### References

- [1] İ. Dökme, Ş. Altındal, Phys. B: Condens. Matter 391 (1) (2006) 59–64.
- [2] T.P. Ma, Semicond. Sci. Technol. 4 (1989) 1061–1079.
- [3] T.P. Ma, P.V. Dressendorfer, Ionizing Radiation Effects in MOS Devices and Circuit, Wiley, New York, 1989.
- [4] E. Atanassova, A. Paskaleva, R. Konakova, D. Spassov, V.F. Mitin, Microelectron. J. 32 (2001) 553–562.
- [5] C.Z. Zhao, S. Taylor, M. Werner, P.R. Chalker, R.J. Potter, J.M. Gaskell, A.C. Jones, J. Vac. Sci. Technol. B 27 (1) (2009) 411–415.
- [6] R.H. Horng, D.S. Wu, J.W. Yu, C.Y. Kung, Thin Solid Films 289 (1–2) (1996) 234–237.
- [7] A.C. Rastogi, R.N. Sharma, J. Appl. Phys. 71 (10) (1992) 5041–5052.
- [8] S.L. Jones, D. Kumar, R.K. Singh, P.H. Holloway, Appl. Phys. Lett. 71 (3) (1997) 404–406.
- [9] S. Zhang, R. Xiao, J. Appl. Phys. 83 (7) (1998) 3842–3848.
- [10] M. Putkonen, T. Sajavaara, L.-S. Johansson, L. Niinistö, Chem. Vap. Deposition 7 (1) (2001) 44–50.
- [11] B.J. Gordon, Solid-State Technol. 36 (1) (1993) 57–61.
- [12] E.K. Evangelou, C. Wiemer, M. Fanciulli, M. Sethu, W. Cranton, J. Appl. Phys. 94 (1) (2003) 318–325.
- [13] H. Fukumoto, T. Imura, Y. Osaka, Appl. Phys. Lett. 55 (4) (1989) 360–361.
- [14] X. Cheng, Z. Qi, G. Zhang, H. Zhou, W. Zhang, M. Yin, Phys. B: Condens. Matter 404 (1) (2009) 146–149.
- [15] P.A. Temple, C.E. Hathaway, Phys. Rev. B 7 (8) (1973) 3685.
- [16] E. Husson, C. Proust, P. Gillet, J.P. Itie, Mater. Res. Bull. 34 (12/13) (1999) 2085–2092.
- [17] E.H. Nicollian, J.R. Brews, MOS Physics and Technology, Wiley, New York, 1982.
- [18] H.N. Lee, Y.T. Kim, S.H. Choh, J. Korean Phys. Soc. 34 (5) (1999) 454–458.
- [19] L.S. Yip, I. Shih, Electron. Lett. 24 (20) (1988) 1287–1289.
- [20] R. Castagné, A. Vapaille, Surf. Sci. 28 (1) (1971) 157–193.
- [21] M. Kuhn, Solid-State Electron. 13 (6) (1970) 873–885.
- [22] W.A. Hill, C.C. Coleman, Solid-State Electron. 23 (9) (1980) 987–993.
- [23] S.M. Sze, Physics of Semiconductor Devices, John Wiley and Sons, Inc., New York, 1981.